A Model Membrane Approach to the Epidermal Permeability Barrier: An X-ray Diffraction Study†

J. A. Bouwstra,*,‡ J. Thewalt,§ G. S. Gooris,‡ and N. Kitson||

Leiden/Amsterdam Center for Drug Research, Gorlaeus Laboratories, Leiden University, P.O. Box 9502, 2300 RA, Leiden, The Netherlands, Division of Dermatology, Department of Medicine, University of British Columbia, 835 West 10th Avenue, Vancouver, British Columbia, Canada, V4Z 4E8, and Department of Physics/Institute of Molecular Biology and Biochemistry, Simon Fraser University, Burnaby, British Columbia, Canada, V5A 1S6

Received November 13, 1996; Revised Manuscript Received April 8, 1997⊗

ABSTRACT: The permeability of mammalian skin is determined in large part by lamellar lipid domains packed between cells of the upper layer of the epidermis, the stratum corneum. Although these lamellae have features in common with typical biological membranes, they differ in having a lipid population composed mainly of ceramides, cholesterol, and free fatty acids. In our initial studies of the relationship between lipid composition and phase behavior in this unusual system, we used deuterium NMR [Kitson *et al.* (1994) *Biochemistry 33*, 6707−6715] to examine aqueous dispersions of nonhydroxylated bovine brain ceramide, cholesterol, and perdeuterated palmitic acid, and found complex phase behavior as a function of temperature and pH, whereas analogous dispersions in which sphingomyelin replaced ceramide resulted in spectra consistent with a fluid lamellar phase under the same conditions. To extend these observations, we examined the same dispersions at pH 5.2 by means of X-ray diffraction. The significant findings are as follows: (1) the ceramide dispersions form complex crystalline phases between room temperature and about 40 °C; (2) the majority of the crystalline cholesterol is not in a separate phase; and (3) the analogous sphingomyelin dispersions form a fluid lamellar phase under the same conditions. We conclude that ceramides, even in the presence of considerable mole fractions of cholesterol, can form crystalline lamellar structures. We suggest that the existence of such structures in stratum corneum may be important in the function of the epidermal permeability barrier, and that the interaction between ceramide and cholesterol in other biological membranes may result in regions having unique physical properties.

A major function of the outermost layer of mammalian epidermis, the stratum corneum, is to provide a barrier between the interior milieu and the external environment. The stratum corneum consists of terminally differentiated cells (the "corneocytes") connected to one another by intercellular junctions, and embedded in a lamellar lipid matrix. A considerable body of evidence supports the hypothesis that the barrier function of the skin is found mainly in these intercellular lipid domains, and that passive diffusion of small molecules (*e.g.*, water, drugs) across the skin occurs predominantly through these regions (Boddé *et al.*, 1989, 1991; Potts & Guy, 1992). It follows that an understanding of the physical properties of this material should help to understand normal and pathological barrier function.

Although the intercellular lipid lamellae possess some features typical of biological membranes, their lipid composition differs markedly from these in being mainly ceramide, cholesterol, and free fatty acid (Wertz *et al.*, 1989, 1991; Schurer & Elias, 1991), and in having, for practical purposes, no phospholipid. Important physiological studies have shown that inhibition of enzymes involved in the synthesis of ceramide, cholesterol, and free fatty acid leads to impaired barrier function (Feingold *et al.*, 1990; Holleran *et al.*, 1991, 1993), strongly suggesting that lipid composition is a key determinant of biological function for these membranes. We believe, as has been suggested previously in more general considerations of lipid diversity in biological membranes (Bloom *et al.*, 1991), that lipid composition may influence membrane function through effects on membrane physical properties. If so, then the very unusual lipid composition of stratum corneum intercellular membranes would be expected to confer equally unusual physical properties.

Some evidence that this is the case has been derived from studies of stratum corneum by small- and wide-angle X-ray diffraction (SAXD and WAXD, respectively).[1] The results may be summarized as follows: (1) In human, pig, and mouse stratum corneum, two lamellar phases are present (Bouwstra *et al.*, 1991, 1992, 1994, 1995; White *et al.*, 1988) having repeat distances of 6 and 13 nm; (2) three lipid chain packings have been found: orthorhombic, hexagonal, and liquid-like (Swanbeck, 1959; Garson *et al.*, 1991; Wilkes *et al.*, 1973). Only the last of these is common in biological membranes. On the other hand, the precursor lipids for SC intercellular membranes (as determined by studies of the

† The financial support of the Natural Sciences and Engineering Research Council of Canada is acknowledged.

* Address correspondence to this author at the Leiden/Amsterdam Center for Drug Research, Gorlaeus Laboratories, Leiden University, P.O. Box 9502, 2300 RA, Leiden, The Netherlands. Telephone: 31-71-274208. Fax: 31-71-274277.

‡ Leiden University.

§ Simon Fraser University.

|| University of British Columbia.

⊗ Abstract published in *Advance ACS Abstracts,* May 15, 1997.

[1] Abbreviations: CER, ceramide; CHOL, cholesterol; PA, palmitic acid; SAXD, small-angle X-ray diffraction; WAXD, wide-angle X-ray diffraction; SC, stratum corneum; q, scattering angle; λ, wavelength; **Q**, scattering vector; d, periodicity.

S0006-2960(96)02812-7 CCC: $14.00

change in lipid composition in mammalian epidermis) consist of more typical membrane lipid classes such as phosphoglycerolipid and sphingolipid (particularly sphingomyelin and monoglycosylceramides) (Squier *et al.*, 1991). With the exception of monoglycosylceramides (Ruocco & Shipley, 1984), these lipids, when combined with cholesterol in aqueous dispersions, form fluid bilayers under conditions of temperature and pH similar to those found *in vivo*. Our working hypothesis therefore is that the systematic change in lipid composition that occurs with mammalian epidermal differentiation results in a radical change in membrane lipid organization. We have previously provided NMR evidence that this is the case (Kitson *et al.*, 1994; Thewalt *et al.*, 1992), and in this study use a complementary technique, X-ray diffraction, to study the same systems at pH 5.2 (approximating the acidic environment of the stratum corneum). Our central findings are as follows: (1) model membranes composed of ceramide, cholesterol, and free fatty acid form lamellar crystalline structures between room temperature and about 40 °C; (2) these lamellae contain cholesterol but do not exhibit solid phase immiscibility; (3) a fluid lamellar phase forms at temperatures above 40 °C; and (4) these phase changes are fully reversible with temperature.

MATERIALS AND METHODS

Lipid and Sample Preparation. Bovine brain sphingomyelin, ceramide-3 (CER), and CHOL were purchased from Sigma (St. Louis, MO) and used without further purification. The acyl chains of sphingomyelin and ceramide obtained from bovine brain were mainly stearic (C18:0), nervonic (C24:1), and lignoceric (24:0). Perdeuterated palmitic acid (PA-d_{31}) was prepared by the method of Hsiao *et al.* (1974). Note that ceramide-3 from bovine brain is structurally similar to the most abundant SC ceramide, ceramide-2.

The dispersions were prepared as described previously (Kitson *et al.*, 1994; Thewalt *et al.*, 1992). Briefly, the lipids were dissolved in benzene/methanol (7:1 v/v) and freeze-dried. The powder was then hydrated at 95 °C in deuterium-depleted water containing 150 mM NaCl, 100 mM citrate, and 4 mM EDTA, pH adjusted to 5.2. In order to achieve homogeneous dispersions, at least 5 freeze−thaw cycles took place between 95 °C and liquid nitrogen temperature.

X-ray Diffraction Measurements. Small-angle X-ray measurements and dynamic wide-angle X-ray measurements were carried out at the Synchrotron Radiation Source at Daresbury Laboratory, U.K., using station 8.2. Specially designed sample holders having two mica windows were used. A detailed description of the equipment has been given elsewhere (Bouwstra *et al.*, 1991). The scattered intensities were measured as a function of **Q**, the scattering vector. The sample−detector distance was set to 1.7 m. Calibration of the detector was carried out with rat tail and CHOL. From the scattering angle, the scattering vector (**Q**) was calculated: $\mathbf{Q} = 4\pi(\sin\theta)/\lambda$, where the wavelength λ is 0.154 nm at the sample position. The final diffraction curves were plotted as a function of **Q**. In this way, a lamellar phase can be characterized by a number of diffraction peaks having the same interpeak spacing. From the positions of the peaks ($\mathbf{Q}_n$), the repeat distance can be calculated by using the equation $\mathbf{Q}_n = 2\pi n/d$, in which d is the repeat distance and n the order of the diffraction peak. The diffraction patterns were normalized with respect to synchrotron beam intensity decay. The data of the static measurements were collected for a period of 15 min. The lipid phase behavior was also measured as a function of temperature. The temperature was increased at a constant heating rate of 2 °C/min, during which the scattered intensity of each curve was collected for 1 min. The temperature was varied between 25 and 95 °C.

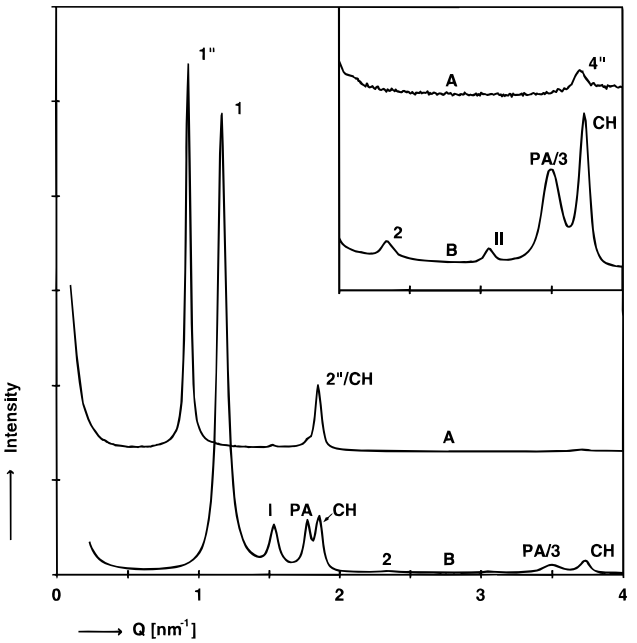

FIGURE 1: Small-angle X-ray diffraction curve of the equimolar sphingomyelin/CHOL/PA dispersion (curve A) and CER/CHOL/PA (curve B) dispersion obtained at room temperature. In the insets to the figure the diffraction curves are plotted at the same **Q**-scaling, but magnified intensity scaling. In the equimolar sphingomyelin dispersion, a periodicity of 6.78 nm (orders indicated by 1″, 2″, and 4″) was found. The weak intensity peaks at 4.11 (1.53 nm^{-1}) and 3.55 nm (1.78 nm^{-1}) are not shown, revealing the weak intensity peaks. The equimolar CER dispersion revealed various phases, with periodicities of 5.38 (orders indicated by 1, 2, and 3), 4.10 nm (orders indicated by I and II), CHOL (indicated by CH), and PA.

Wide-Angle X-ray Diffraction. The diffraction patterns were obtained with a fiber diffraction camera at station 7.2 of the synchrotron radiation source in Daresbury. A more detailed description of this instrument is given elsewhere (Bouwstra *et al.*, 1992). The positions of the reflections will be denoted by their spacings in real space. The X-ray path length through the sample was 1 mm. The temperature of the sample could be adjusted between 25 and 120 °C, with the read-out thermocouple inserted in the sample cell. The sample to film distance was set to 0.11 m, and the wavelength of the X-rays at the position of the sample was 0.1488 nm.

RESULTS

Long-Range Ordering. The diffraction patterns obtained at room temperature using equimolar dispersions of CER, CHOL, and PA or sphingomyelin, CHOL, and PA are given in Figure 1. The spacings and the corresponding phases are summarized in Table 1. A detailed explanation is given below.

We first consider the phase behavior of the equimolar sphingomyelin dispersion. The dominant feature consists of three diffraction peaks located at $\mathbf{Q} = 0.927$, 1.848, and 3.70 nm^{-1}. These reflections can be interpreted as being the first, second, and fourth orders of a lamellar phase with a periodicity of 6.78 nm. In addition, a low-intensity reflection was observed at $\mathbf{Q} = 1.53$ nm^{-1} (spacing 4.11 nm), also

Table 1: Reflections and Interpretation of the Equimolar Sphingomyelin/CHOL/PA and CER/CHOL/PA Dispersions[a]

temp (°C)	phases: spacing (in nm) followed by diffraction peak order	interpretation
	Sphingomyelin Dispersion	
20	6.78 nm phase: 6.78(1), 3.40(2), 1.70(4)	L
	3.55 nm phase: 3.55(1)**	UNK
	4.11 nm phase: 4.11(1)**	UNK
30	6.70 nm phase: 6.70(1), 3.35(2), 1.68(4)	L
40	6.63 nm phase: 6.63(1), 3.30(2), 1.66(4)	L
50 and 58	6.60 nm phase: 6.60(1), 3.30(2), 1.65(4)	L
68	6.55 nm phase: 6.55(1), 3.29(2), 1.65(4)	L
	CER Dispersion	
25 and 35	5.38 nm phase: 5.38(1), 2.69(2), 1.80(3), 1.36(4)	L
	4.10 nm phase: 4.10(1), 2.05(2), 1.03(4)	L
	PA*: 3.55(1), 1.78(2), 1.18(3)	M
	CHOL: 3.35(1), 1.68(2), 1.12(3)	TRI
40	5.34 nm phase: 5.34(1), 2.67(2), 1.79(3), 1.35(4)	L
	4.21 nm phase: 4.21(1), 2.10(2), 1.39(3), 0.813(5)	L***
	4.10 nm phase: 2.05(2)	L
	PA**: 3.55(1), 1.78(2), 1.18(3)	M
	CHOL**: 3.35(1), 1.68(2)	TRI
50	5.34 nm phase: 5.34(1)	L
	4.27 nm phase: 4.27(1), 2.12(2), 1.40(3), 1.05(4), 0.834(5)	L
	4.10 nm phase: 2.05(2)	L
60	4.17 nm phase: 4.17(1), 2.06(2), 1.38(3)	L
70	4.09 nm phase: 4.09(1), 2.05(2)	L
	diffuse peak at 3.36 nm	UNK
80	4.4 nm phase: 4.04(1)	L
	diffuse peak at 3.27 nm	UNK
90	no peaks	

[a] (*) The interpretation of PA is not completely sure; (**) the 3.38 and 3.55 nm reflections disappeared between 40−50 and 50−58 °C, respectively; (***) interpretation is based on SAXD and WAXD results. L = lamellar, UNK = unknown, TRI = triclinic, M = monoclinic. The reflections were observed by SAXD.

present in the diffraction pattern of the CER dispersion (see below), and a small shoulder at $\mathbf{Q} = 1.79$ nm^{-1} (3.55 nm). The 3.55 nm peak coincides with the strongest peak in the diffraction curve of PA and might therefore indicate that a small amount of the PA phase-separated.

In contrast, the equimolar CER dispersion has a very complicated diffraction pattern (see Figure 1). It is obvious that at room temperature several phases coexist in the dispersion. At $\mathbf{Q} = 1.17$ nm^{-1}, a very strong diffraction peak is present corresponding to a 5.38 nm spacing. Since second-, third-, and fourth-order reflections are located at 2.69, 1.80, and 1.35 nm ($\mathbf{Q} = 2.31$, 3.49, and 4.62 nm^{-1}, respectively), these reflections are most likely based on a lamellar phase with a periodicity of 5.38 nm. (The identification of the 1.80 nm peak was uncertain, since this peak could also be assigned to polycrystalline PA, as discussed below.)

A second phase, a minor component with a repeat distance of 4.10 nm, was also present. This was concluded from the presence of first- and second-order diffraction peaks at 4.10 nm spacing ($\mathbf{Q} = 1.52$ nm^{-1}) and 2.05 nm spacing ($\mathbf{Q} = 3.05$ nm^{-1}). That these peaks are based on the same phase was confirmed by measurements carried out as a function of temperature as described below. The third-order reflection is expected to be located at a position corresponding to a 1.37 nm spacing, but this is approximately the same position as the fourth-order reflection of the 5.38 nm phase (see above). From examining the phase behavior as a function of temperature as discussed subsequently, we could deduce that the observed 1.35 nm reflection was in fact connected with the 5.38 nm phase.

Furthermore, two partially resolved peaks were observed at spacings of 3.54 nm ($\mathbf{Q} = 1.77$ nm^{-1}) and 3.38 nm ($\mathbf{Q} = 1.86$ nm^{-1}). The latter diffraction peak and the peak at 1.68 nm ($\mathbf{Q} = 3.74$ nm^{-1}) were most likely due to a small amount of CHOL that separated as CHOL monohydrate crystals. This was confirmed by the wide-angle X-ray diffraction patterns as discussed below. The 3.54 nm diffraction peak was more difficult to interpret. It might be that part of the PA crystallized in a separate phase. Polycrystalline PA results in diffraction peaks at 3.51 nm—in good agreement with our observed 3.54 nm spacing—and 1.76 nm. However, although at a spacing of approximately 1.80 nm a broad peak was observed, confirming the possible presence of PA crystals, no definite conclusions could be drawn since this peak could also be identified as the third-order reflection of the 5.38 nm phase (see above), and both the 5.38 nm reflections and the 3.54 nm peak disappear between 40 and 50 °C.

Another possible interpretation of the equimolar CER SAXD pattern is that a 10.7 nm lamellar phase is present, having a third-order reflection at 3.54 nm and a second-order one at 5.38 nm. Such a long periodicity is not unusual for CER dispersions and was found by Parrott and Turner (1993) in unhydrated dispersions of CER and CHOL and by Bouwstra *et al.* (1996) in hydrated dispersions of isolated ceramides and cholesterol at pH 5.0. However, the information we obtained as a function of temperature (see below) excluded the possibility of a 10.7 nm phase: between 30 and 40 °C, the ratio of the intensities of the 3.54 nm and 5.38 nm peaks increased dramatically.

Long-Range Ordering as a Function of Temperature. The measurements at various temperatures were carried out *statically* and *dynamically*. In the static measurements, each curve represents data collected for 15 min at each distinct temperature. These measurements were performed for peak assignment in which the weak intensity peaks play an important role. For the dynamic measurements, the temperature was increased at a constant rate of 2 °C/min, during which the data were collected. Every minute a new diffraction curve was obtained. The advantage of these dynamic measurements is that one obtains detailed information on phase changes as a function of temperature. Furthermore, dynamic measurements facilitate the correlation between phase transitions detected with wide- and small-angle X-ray diffraction.

We first consider the sphingomyelin/CHOL/PA dispersion. Static measurements were carried out for temperatures between 20 and 68 °C. As the temperature was increased, the three diffraction peaks associated with the dominant 6.78 nm lamellar phase gradually shifted to higher **Q**-values, resulting in a 6.55 nm lamellar phase at 68 °C (see Table 1). The weak 4.11 nm peak disappeared between 40 and 50 °C, while the 3.55 nm shoulder disappeared between 50 and 58 °C.

The results of the static and dynamic measurements of the equimolar CER/CHOL/PA dispersion are presented in Figures 2 and 3, respectively. The changes observed in the diffraction pattern of the CER dispersion as a function of temperature were complex. We summarize the static measurements first. At 35 °C, the diffraction pattern was similar to that at 25 °C, but between 35 and 40 °C, it began to change. The 5.38 nm peak shifted to a spacing of 5.34 nm

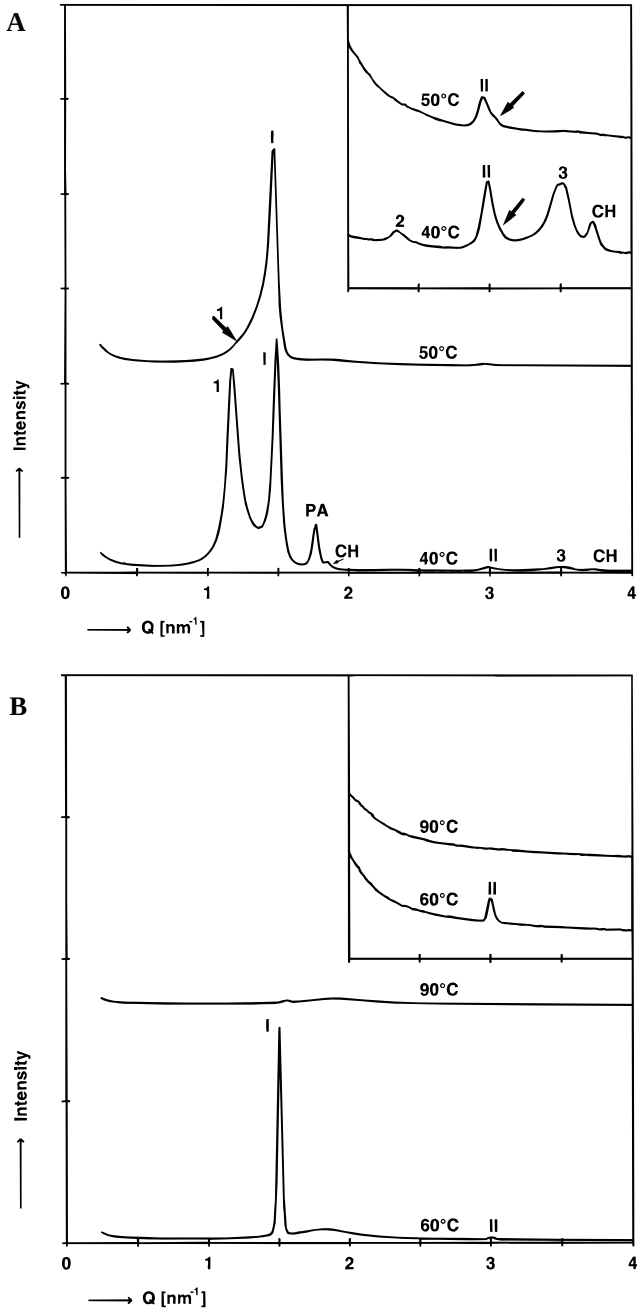

FIGURE 2: (A) Small-angle diffraction curves of the equimolar CER/CHOL/PA dispersion at 40 and 50 °C. The temperatures are given in the figure. See Figure 1 for the identification of peaks. A small peak was found at 2.05 nm (see arrow), indicating that some lipids were still present in the 4.10 nm phase. (B) Small-angle diffraction curves of the equimolar CER/CHOL/PA dispersion at 60 and 90 °C. For identification of the peaks, see Figure 1.

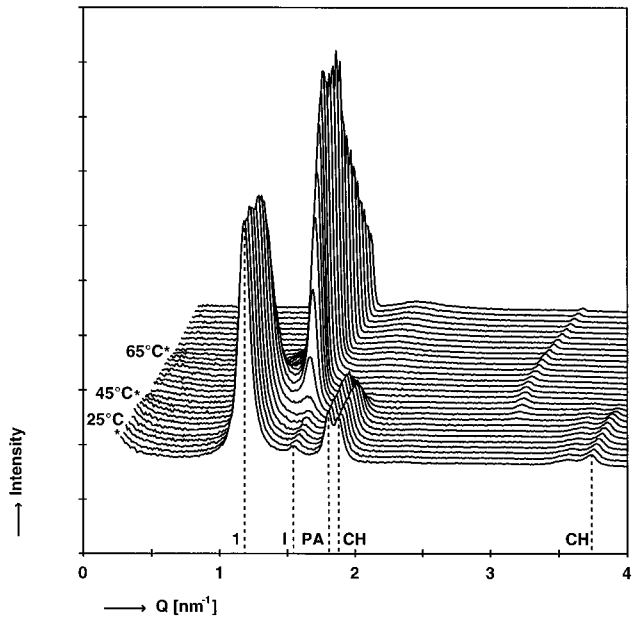

FIGURE 3: Small-angle X-ray diffraction curves for the equimolar CER/CHOL/PA dispersion as a function of temperature. The heating rate was 2 °C/min; the temperature range is 25−81 °C. The temperatures are indicated in the figure. See Figure 1 for identification of the peaks.

and decreased in intensity over this temperature range. Furthermore, between 35 and 40 °C, the 4.10 and 2.05 nm peaks both increased in intensity and shifted to 4.21 and 2.10 nm, respectively, *i.e.*, a longer repeat spacing. This observation confirms that the 4.10 and 2.05 nm peaks were indeed associated with the same phase. The 3.38 and 1.68 nm peaks, due to crystalline CHOL monohydrate, weakened in this temperature range and disappeared between 40 and 50 °C. From 35 to 40 °C, the 3.55 nm peak did not change in position, nor did its intensity diminish as did the intensity of the 5.34 nm peak; thus, a 10.7 nm 'double bilayer' phase is not present. The most likely explanation for the 3.55 nm peak is that a small amount of PA has phase-separated. From the diffraction curves collected during the dynamic measurements (Figure 3), it is clear that the repeat spacing of the 4.10 nm phase increased to 4.21 nm between 37 and 41 °C, and to 4.27 nm by 51 °C. At higher temperatures the 4.27 nm peak dominates all other phases: between 49 and 53 °C, the 5.34 and 3.55 nm peaks essentially disappeared. These results agree with the static measurements: at 50 °C (Figure 2B), one strong 4.27 nm phase was present in the lipid mixture, whose diffraction peak positions shifted from 4.21 and 2.10 nm at 40 °C to 4.27 and 2.13 nm, respectively. At 50 °C, the 4.27 nm peak was asymmetric due to a small shoulder caused by the presence of a small amount of lipids organized in the 5.34 nm phase. The reflection at 1.41 nm spacing ($\mathbf{Q} = 4.46$ nm^{-1}) could be interpreted as the third-order peak of the 4.27 nm phase. In the wide-angle pattern, the fourth- and fifth-order reflections of the 4.27 nm phase were found at 50 °C, confirming that the 4.27 nm phase is lamellar. Between 50 and 80 °C, the repeat distance of the 4.27 nm phase gradually decreased to 4.05 nm. No other phases were present in this temperature range, and the 4.05 nm phase disappeared between 80 and 90 °C.

Short-Range Ordering at Room Temperature. The diffraction pattern of the equimolar dispersion of sphingomyelin/CHOL/PA (not shown) indicated that the majority of lipid chains were packed as liquid hydrocarbons. It also exhibited some very weak reflections, indicating the presence of a negligible proportion of crystalline structure.

A large number of reflections were found in the diffraction pattern of the equimolar dispersion of CER/CHOL/PA (see Figure 4). Several diffraction rings were based on CHOL-monohydrate, that is characterized by three high-intensity rings at 0.592 and 0.586 and a large number of very weak (vw), weak (w), or medium (m) intensity rings with spacings of 0.555(w), 0.532(w), 0.494(w), 0.482(vw), 0.471(vw), 0.454(vw), 0.384(w), and 0.377(m) nm, respectively. Most of the reflections were weak or very weak, indicating that only a small amount of CHOL coexisted in CHOL-monohydrate form. No features indicating the presence of a liquid phase were found in the diffraction pattern. The

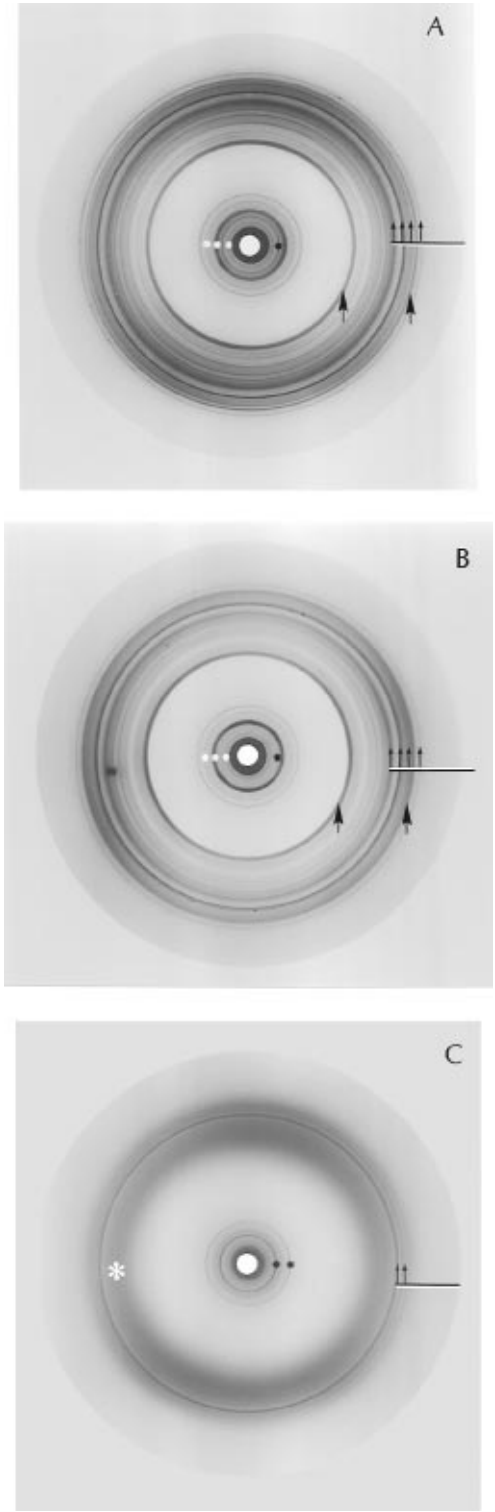

FIGURE 4: Wide-angle X-ray diffraction pattern for the equimolar CER/CHOL/PA dispersion at 25 °C (A), 40 °C (B), and 50 °C (C). (A and B) The black asterisk indicates the 2.05 (25 °C) and 2.11 (40 °C) nm spacing of the 4.1 and the 4.2 nm phase, respectively. The white asterisks refer to the higher order reflections of the 5.38 nm phase. The large arrows indicate the strongest cholesterol reflections, while the small arrows indicate the reflections based on the crystalline lateral packing of the lipids (spacing 0.429, 0.406, 0.395, and 0.364 nm). (C) Small arrows: the spacings based on the gel and crystalline packing. Black asterisks: higher order reflections based on the 4.2 nm lamellar phase. The big white asterisk indicates the broad reflection based on the liquid lateral packing.

remaining reflections due to the hydrocarbon packing of the lipids were located at 0.464(w), 0.441(w), 0.429(m), 0.406-(m), 0.395(w), and 0.364(w) nm. It is likely that the reflection at 0.377 nm not only was due to crystalline CHOL but also could be attributed to the lateral hydrocarbon packing. With this limited information and the complex phase behavior of the system, it is very difficult to assign the lipid reflections to a particular sublattice, but the spacings strongly indicate that various crystalline phases coexist in the dispersion. For example, a triclinic subcell gives rise to short spacings at 0.37, 0.39−0.404, and 0.44−0.46 nm, which is rather close to the 0.364, 0.395, 0.406, 0.441, and 0.464 nm spacings in the diffraction pattern. It is therefore not unlikely that the triclinic sublattice is present. However, the reflection at 0.429 nm cannot be attributed to a triclinic subcell, but might be explained by a monoclinic one. The monoclinic sublattice gives rise to reflections at spacings of approximately 0.37, 0.43, and 0.46 nm.

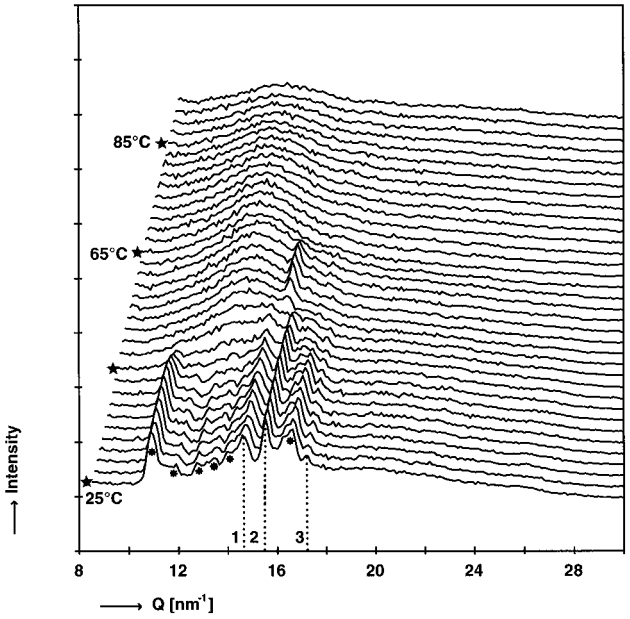

FIGURE 5: Wide-angle measurements as a function of temperature for the equimolar CER/CHOL/PA dispersion, measured dynamically between 25 and 93 °C using a heating rate of 2 °C/min. The asterisks indicate the CHOL reflections. 1, 2, and 3 indicate the reflections at 0.429, 0.406, and 0.364 nm, respectively. Note the appearance of the 0.42 nm reflection between around 49 and 65 °C, indicating the presence of a hexagonal lateral packing.

Short-Range Ordering as a Function of Temperature. The diffraction patterns were obtained *statically* by measuring the pattern at distinct temperatures using film detection and *dynamically* by measuring the diffraction curves at a constant heating rate of 2 °C/min using electronic detection. The dynamic measurements were performed in order to follow the phase changes as a function of temperature whereas the static measurements were carried out to detect weak diffraction rings and to obtain high-resolution diffraction patterns. The results of the static (short spacing resolution 0.002 nm) and dynamic measurements (short spacing resolution 0.01 nm) are shown in Figures 4 and 5, respectively. The spacings are given in Table 2. We first consider the diffraction patterns at distinct temperatures. Between 25 and 40 °C, no changes in the positions of reflections based on lateral packing were observed. At 40 °C, one additional reflection was observed at 2.10 nm spacing, being the second-order reflection of the 4.21 nm phase. This confirms the results of the small-angle measurements. Between 40 and 50 °C, the cholesterol reflections decreased in intensity, and the change in the diffraction pattern was obvious. Most of the reflections disappeared or became very weak in intensity.

Table 2: Short-Range Ordering of the Equimolar CER Dispersion as a Function of Temperature[a]

temp (°C)	short-range ordering
25, 35	lateral packing: 0.464[w], 0.441[w], 0.429[m], 0.406[m], 0.395[w], 0.364[w]
	definite CHOL reflections
40	lateral packing: see 25, 35 °C
	CHOL reflections more diffuse
50	lateral packing: 0.45[m], 0.415[m], 0.406[w], 0.396[w], 0.367[w]
	no CHOL reflections
59	lateral packing: 0.45[s]
71	lateral packing: 0.45[s]

[a] The reflections are detected by WAXD.

At 50 °C, a medium 0.415 nm reflection due to a hexagonal hydrocarbon sublattice was present, and three low-intensity rings were observed at 0.396, 0.367, and 0.406 nm, indicating that a small part of the lipids were still in a crystalline state. Furthermore, at 50 °C, a broad band was observed at a spacing of approximately 0.45 nm, which is due to liquid lateral lipid chain packing. It appears that at 50 °C, crystalline, hexagonal, and liquid hydrocarbon packings coexist in the dispersion. The changes in lateral packing between 40 and 50 °C were confirmed by the dynamic measurements. As well, the dynamic measurements showed that upon further heating the intensity of the 0.415 nm reflection first increased (between 51 and 57 °C) and then decreased until the reflection disappeared at approximately 65 °C.

DISCUSSION

In previous deuterium NMR studies (Kitson *et al.*, 1994; Thewalt *et al.*, 1992) of equimolar sphingomyelin/CHOL/PA dispersions (in which PA served as the probe), only spectra characteristic of fluid lamellae were found between 20 and 75 °C. The X-ray diffraction results presented in this paper are in keeping with these, conclusively demonstrating that sphingomyelin/CHOL/PA exists almost entirely as a single lamellar phase having liquid hydrocarbon chain packing and a repeat spacing of 6.78 nm (that, as expected, decreases slightly as a function of increasing temperature). This is consistent with what has been described as the "liquid ordered" phase (Ipsen *et al.*, 1989) which is widely found in membranes containing substantial amounts of cholesterol, and also with the "fluid mosaic" model of cellular membranes proposed by Singer and Nicolson (1972). Our results are also consistent with other model membrane studies such as that of McIntosh *et al.* (1992a,b), who found that an equimolar mixture of tetracosanoylsphingomyelin and cholesterol formed a lamellar phase having liquid lipid chain packing and a periodicity ranging between 5.93 and 6.63 nm. The latter variation depended on the applied vapor pressure, and we believe our larger repeat distance is due to the presence of excess buffer solution in our dispersions.

In contrast, the analogous dispersions containing ceramide were found to display complex polymorphism as a function of temperature, again consistent with previous ^{2}H NMR experiments. The SAXD results showed a dominant lamellar phase at room temperature having a repeat spacing of 5.38 nm, together with smaller diffraction peaks attributed to crystalline PA and cholesterol monohydrate, as well as two minor peaks probably due to a lamellar phase having a repeat spacing of 4.10 nm. The WAXD results indicated the presence of more than one crystalline lipid organization, but

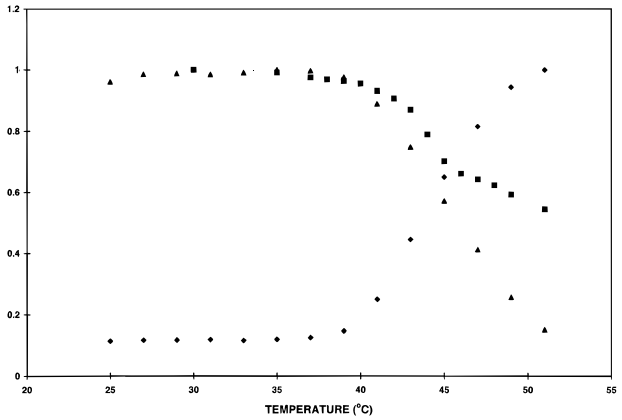

FIGURE 6: Equimolar CER/CHOL/PA dispersions: comparison of SAXD and ^{2}H NMR results. The temperature dependence of the height of the first-order SAXD peak representing lamellae with repeat spacing of 5.38 nm (triangles) and 4.10−4.27 nm (diamonds). Squares: The temperature dependence of the average width of the ^{2}H NMR spectrum as reported by deuterated PA.

no evidence for liquid or hexagonal packings typical of, respectively, liquid ordered and gel phase bilayers. However, the NMR observations of the same dispersions under the same conditions showed that at least some of the lipid probe was in a more mobile phase (Kitson *et al.*, 1994), and perhaps there was insufficient lipid to be detected by WAXD under these conditions. The 4.10 nm lamellar phase may be due to a small amount of more fluid lipid coexisting with the larger crystalline phases in the lower temperature range, but this has not been confirmed by WAXD.

The molecular organization of the 5.38 nm lamellar phase cannot be precisely defined as yet. This phase disappears between approximately 40 and 50 °C (except for a weak shoulder at 50 °C), the same temperature range over which the WAXD crystalline reflections all but disappear. The temperature of the CER/CHOL/PA dispersion's chain- and lattice-melting transition, measured using ^{2}H NMR, also coincides with the disappearance of the 5.38 nm phase (Figure 6). Thus, this phase appears to consist of layers of crystalline lipids, containing ceramides and the major proportion of PA and CHOL, without evidence for immiscibility. A partially interdigitated bilayer, where the long ceramide chains oppose either short ceramide chains, PA, or CHOL, would be consistent with the observed repeat spacing, especially if the headgroups of neighboring layers are in close apposition. The latter is likely to occur, since as a function of hydration level no swelling of the lamellae in stratum corneum occurred (Bouwstra *et al.*, 1991).

The lipid organization in the low-intensity 4.10 nm phase is difficult to assess due to the limited information available: only two reflections were present that could be unambiguously assigned to this phase. (More reflections might be present but were obscured by reflections from the other phases.) No further attempts were undertaken to assign these peaks to a particular structure, but the most likely interpretation is lamellar. However, the molecular arrangement of this phase is unclear, since its repeat distance is rather small for a bilayer phase even if we assume the absence of a thick aqueous layer between lamellae. This short periodicity may result from interdigitation of the hydrocarbon chains, as has been found for lipid systems with large differences in hydrocarbon chain lengths (Lewis *et al.*, 1994; Mattai *et al.*, 1987; McIntosh *et al.*, 1984). Alternatively, since the CER mainly contains stearic and nervonic acids, the 4.10

nm phase might be an enriched CER fraction having chain length C18, while the 5.38 nm phase might be enriched with CR having a chain length of 24. Finally, if a correspondence exists between this 4.10 nm structure and the noncrystalline lipids NMR shows to be in the dispersion, trans−gauche isomerization would account for some further reduction in lamellar thickness compared with the 5.38 nm phase.

Above 37 °C, a lamellar phase having a 4.21 nm repeat distance was formed, and above 40 °C this increased to 4.27 nm. This was unexpected: bilayers usually become thinner as they are heated due to increasing chain disorder. A probable explanation is that the concentration of CHOL in these lamellae increases over this temperature range, causing the lipid chains to stretch. The source of the extra CHOL is presumably CHOL monohydrate, which largely disappears between 40 and 50 °C. Alternatively, ceramide having longer chains may progressively melt into the fluid bilayer over this temperature range (the 5.34 nm reflection all but disappears by 50 °C), thereby increasing the repeat spacing. At higher temperatures, the lamellae thin gradually, as is normally found, until at approximately 70 °C the repeat spacing is just 4.09 nm. It is interesting to compare the lamellar repeat spacing found in the sphingomyelin/CHOL/PA dispersion (6.60 nm) with that found for the CER/CHOL/PA dispersion (4.27 nm) at 50 °C. Our previous ^{2}H NMR results show the PA chain order parameter profiles to be nearly identical at this temperature, which implies that the major reason for the different observed repeat spacings in the two dispersions is a difference in the thickness of their polar headgroup and aqueous layers. We can conclude that at 50 °C the sphingomyelin/CHOL/PA lamellae are about 2.3 nm thicker in this region than their CER/CHOL/PA counterparts.

In parallel with the changes in long-range order, changes in lipid packing were observed with increasing temperature. Between 40 and 50 °C, both liquid and hexagonal patterns appeared (corresponding to, respectively, fluid ordered and gel phase bilayers), and at 50 °C only a very small portion of the lipid was crystalline. This corresponds well to ^{2}H NMR observations at 50 °C that show only a small proportion of "solid" PA (Kitson *et al.*, 1994) or CHOL (Fenske *et al.*, 1994) remaining. Despite the complexity of this three component system then, we see that between room temperature and 37 °C there is one predominant lipid lamellar structure having a repeat distance of 5.38 nm and a complex crystalline packing, and which incorporates all three major lipid classes without evidence for solid phase immiscibility. Above 37 °C, there is a gradual melt until by 50 °C the predominant lipid phase has a repeat spacing of 4.27 nm and a liquid lipid packing, and again contains cholesterol (Fenske *et al.*, 1994), palmitic acid (Kitson *et al.*, 1994), and also ceramide (Thewalt *et al.*, 1992). Above 60 °C, there was evidence in both NMR and X-ray studies for the gradual disappearance of the lamellar phase and the growth of a highly mobile fluid phase which was isotropic on the NMR time scale without showing evidence for reflections characteristic of a cubic phase. Preliminary freeze−fracture evidence suggests that small vesicles may form (S. Bayerl and N. Kitson, unpublished observations). It is important to point out that all observed changes are thermally reversible.

Although ceramides have received relatively little attention in studies of biological membrane models, there is a considerable literature concerning their phase behavior, particularly from the pioneering work of Irmin Pascher and his colleagues (Lofgren & Pascher, 1977; Dahlén & Pascher, 1979). More recently, Parrott and Turner (1993) studied the phase behavior of unhydrated dispersions prepared from ceramide and CHOL. In the context of stratum corneum intercellular membranes, Abraham and Downing (1988) examined hydrated dispersions of epidermal ceramide, cholesterol, and palmitic acid; Blume *et al.* (1993) made aqueous dispersions from bovine brain ceramide, cholesterol, cholesterol sulfate, and palmitic acid whereas Lieckfeldt *et al.* (1993), Schuckler *et al.* (1993), and Friberg *et al.* (1987) used more complex mixtures prepared from ceramides, CHOL, free fatty acids, and di- and triglycerides. In all of this work, crystalline lipid phases, as reported for our models, were not invariably found. The reasons for this discrepancy are not entirely clear, but sufficient numbers of differences exist among the studies in sample preparation and technique to make direct comparisons difficult. However, we believe that our results are of relevance to understanding SC intercellular membranes for several reasons.

First, it seems clear that the CER/CHOL/PA dispersions will form lamellar phases despite the absence of conventional membrane hydrophilic headgroups on any of the lipids. At lower temperatures (less than about 40 °C), most of the intensity is found in a phase having a repeat distance of 5.38 nm. A comparable lamellar phase with a repeat spacing of approximately 5.2 nm has been observed in mixtures prepared from pig ceramides and CHOL (Bouwstra *et al.*, 1996). There is no evidence, however, for the "longer" repeat distance of 10−13 nm as reported for lamellar phases in mammalian stratum corneum (Bouwstra *et al.*, 1991, 1992, 1994, 1995; White *et al.*, 1988) or in dry mixtures prepared from isolated stratum corneum lipids (Parrott & Turner, 1993). Bouwstra *et al.* (1996) examined the phase behavior of dispersions of isolated ceramides and cholesterol and found, at room temperature, two lamellar phases having periodicities of 5.2 and 12.2 nm, similar to those of intact stratum corneum. One explanation for our failure to observe the longer repeat spacing in our dispersion might be its relative simplicity of composition: in stratum corneum, at least six different classes of ceramides are present together with a variety of free fatty acids, while our CER/CHOL/PA dispersion was prepared from only one type of CER (albeit corresponding to SC CER-2, the most abundant) and one free fatty acid. Interesting similarities between the results presented here and those of Bouwstra *et al.* (1996) are observed at higher temperatures: both studies show that at approximately 40−45 °C a new lamellar phase with a periodicity of 4.2 nm was formed which dominated the diffraction curve as the sample was heated. To fully understand the differences and similarities between lipid phase behavior in the various CER dispersions and in the stratum corneum will require further research.

Second, these experiments show that phase behavior may be more complex than found with a single technique. Below about 40 °C, the major lipid packing is crystalline, and two lamellar phases appear to coexist. This is consistent with NMR results in the same temperature range showing extremely limited molecular motion on the ^{2}H NMR time scale, and no measurable lateral diffusion (Kitson *et al.*, 1994), but the coexistence of lamellar phases is not detectable with NMR. Furthermore, a phase having liquid chain packing is detectable by WAXD as a diffuse band at 0.45 nm, but may be obscured at low concentrations and is not

clearly observable coexisting with the crystalline phases in our experiments at these temperatures. However, the NMR subtraction experiments [see Figure 7 in Kitson *et al.* (1994)] showed definitively that a small amount of the palmitic acid probe was present in a fluid phase (the probe was undergoing axially symmetric motion on the NMR time scale). Thus, the organization of tissue lipid may be more complex than shown by one technique, and the extent and organization of a minor component (*e.g.*, the fluid phase) may have considerable biological importance.

Finally, the existence of a crystalline phase (in which membrane lipids are organized on a lattice and have extremely reduced lateral and rotational mobility compared to the fluid arrangement of other mammalian cellular membranes) has been demonstrated in stratum corneum, and shown in our admittedly imperfect models to be dependent on the presence of ceramides and strongly influenced by temperature and pH. As has been discussed elsewhere (*e.g.*, Kitson *et al.*, 1994; Forslind, 1994; Haines, 1994), such a phase would be expected to radically alter membrane physical properties (such as permeability) in comparison with the fluid phase. Thus, we suggest that the complex lipid modifications that are characteristic of epidermal differentiation may have evolved to produce biological membranes that are much more effective barriers (*e.g.*, to water) than are typical fluid membranes. As a corollary, we point out that ceramides, the membrane lipids apparently critical to the formation of such crystalline phases, are enzymatically derived in a fluid lipid matrix from sphingolipids such as sphingomyelin and glucosylceramide. The difficulties in forming crystalline domains from fluid membranes containing a high concentration of cholesterol may have been overcome through the apparent ability of cholesterol to incorporate itself in some fashion into these domains with ceramide without phase separation. This to our knowledge is a radical departure from the behavior of cholesterol with other membrane lipids and, given the newly appreciated biological roles for ceramide, deserves further consideration. In a study of a semisynthetic cerebroside (*N*-palmitoylgalactosylsphingosine) and cholesterol, Ruocco and Shipley (1984) found solid phase immiscibility between these lipids in hydrated dispersions at temperatures less than about 40 °C. On the other hand, Skarjune and Oldfield (1979) found clear evidence for the formation of a limited fluid lamellar phase in hydrated dispersions of the same two lipids (1:1 mol/mol) at room temperature, in addition to a gel phase. However, in neither study was there evidence for a solid or crystalline phase containing both cholesterol and sphingolipid.

The behavior of ceramide with cholesterol in other biological membranes may also be of interest. Recent research indicates that ceramide, produced by sphingomyelinase in response to various extracellular signals, acts as a second messenger in inducing growth arrest and "programmed cell death" or apoptosis [*e.g.*, see Obeid and Hannun (1995)]. Given the behavior of ceramide with cholesterol in our experiments, it is conceivable that local increases in ceramide concentration in cellular membranes (at the expense of sphingomyelin) may lead to significant alterations in membrane physical properties in the same regions. We believe that such alterations would have physiological significance, and deserve consideration in further studies of the ceramide second-messenger hypothesis.

ACKNOWLEDGMENT

X-ray diffraction measurements were made at Daresbury Laboratory station 8.2 which was built as part of a NWO/SERC agreement. ^{2}H NMR measurements were performed at the University of British Columbia, Vancouver, B.C., Canada, with the generous support of Prof. Myer Bloom.

REFERENCES

Abraham, W., Wertz, P. W., & Downing, D. T. (1988) *Biochim. Biophys. Acta 939*, 403−408.
Bloom, M., Evans, E., & Mouritsen, O. G. (1991) *Q. Rev. Biophys. 24*, 293−397.
Blume, A., Jansen, M., Ghyczy, M., & Gareiss, J. (1993) *Int. J. Pharm. 99*, 219−228.
Boddé, H. E., Kruithof, M. A. M., Brussee, J., & Koerten, H. K. (1989) *Int. J. Pharm. 253*, 13−24.
Boddé, H. E., van den Brink, I., Koerten H. K., & de Haan, F. H. N. (1991) *J. Controlled Release 15*, 227−236.
Bouwstra, J. A., Gooris, G. S., van der Spek, J. A., & Bras, W. (1991) *J. Invest. Dermatol. 97*, 1004−1012.
Bouwstra, J. A., Gooris, G. S., van der Spek, J. A., & Bras, W. (1992) *Int. J. Pharm. 84*, 205−216.
Bouwstra, J. A., Sibon, O., Salomons-de Vries, M. A., Hofland, H. E. J., & Spies, F. (1993) *Proc. Int. Symp. Controlled Release Bioact. Mater., 19*, 481−482.
Bouwstra, J. A., Gooris, G. S., van der Spek, J. A., Lavrijsen, S., & Bras, W. (1994) *Biochim. Biophys. Acta 1212*, 183−192.
Bouwstra, J. A., Gooris, G. S., Bras, W., & Downing, D. T. (1995) *J. Lipid Res. 36*, 685−695.
Bouwstra, J. A., Gooris, G. S., Cheng, K., Weerheim, A., Bras, W., & Ponec, M. (1996) *J. Lipid Res. 37*, 999−1011.
Dahlén, B., & Pascher, I. (1979) *Chem. Phys. Lipids 24*, 119−133.
Fartasch, M., Bassakas, I. D., & Diepgen, T. L. (1992) *Br. J. Dermatol. 127*, 221−227.
Feingold, K. R., Mao-Qiang, M., Menon, G. K., Cho, S. S., Brown, B. E., & Elias, P. M. (1990) *J. Clin. Invest. 86*, 1738−1745.
Fenske, D. B., Thewalt, J. L., Bloom, M., & Kitson, N. (1994) *Biophys. J. 67*, 1562−1573.
Forslind, B. (1994) *Acta Derm.-Venereol. 74*, 1−6.
Friberg, S., Suhaimi, H., & Goldsmidt, L. (1987) *J. Dispersion Sci. Technol. 8*, 173−178.
Garson, J. C., Doucet, J., Leveque, J. L., & Tsoucaris, G. (1991) *J. Invest. Dermatol. 96*, 43−49.
Grubauer, G., Feingold, K. R., & Elias, P. M. (1987) *J. Lipid Res. 28*, 746−752.
Haines T. H. (1994) *FEBS Lett. 346*, 114−122.
Holleran, W. M., Mao-Qiang, M., Gao, W. N., Menon, G. K., Elias, P. M., & Feingold, K.R. (1991) *J. Clin. Invest. 88*, 1338−1345.
Holleran, W. M., Takagi, Y., Menon, G. K., Legler, G., Feingold, K. R., & Elias, P. M. (1993) *J. Clin. Invest. 91*, 1656−1664.
Hsiao, C. Y. Y., Ottaway, C. A., & Wetlaufer, D. B. (1974) *Lipids 9*, 913−915.
Ipsen, J. H., Mouritsen, O. G., & Zuckermann, M. (1989) *Biophys. J. 56*, 661−667.
Kitson, N., Thewalt, J., Lafleur, M., & Bloom, M. (1994) *Biochemistry 33*, 6707−6715.
Lewis, R. N. A. H., McElhaney, R. N., Monck, M. A., & Cullis, P. R. (1994) *Biophys. J. 67*, 197−207.
Lieckfeldt, R., Villavain, J., Gomez-Fernandez, J. C., & Lee, G. (1993) *Biochim. Biophys. Acta 1151*, 182−188.
Löfgren, H., & Pascher, I. (1977) *Chem. Phys. Lipids 20*, 273−284.
Mattai, J., Scripada, P. K., & Shipley, G. G. (1987) *Biochemistry 26*, 3287−3297.
McIntosh, T. J., Simon, S. A., & Porter, N. A. (1984) *Biochemistry 23*, 4038−4044.
McIntosh, T. J., Simon, S. A., Needham, D., & Huang, C. (1992a) *Biochemistry 31*, 2012−2020.
McIntosh, T. J., Simon, S. A., Needham, D., & Huang, C. (1992b) *Biochemistry 31*, 2020−2024.
Obeid, L. M., & Hannun, Y. A. (1995) *J. Cell. Biochem. 58*, 191−198.

Parrott, D. T., & Turner, J. E. (1993) *Biochim. Biophys. Acta 1147*, 273−276.
Potts, R. O., & Guy, R. H. (1992) *Pharm. Res.* 9, 663−669.
Ruocco, M. J., & Shipley, G. G. (1984) *Biophys. J. 46*, 695−707.
Schuckler, F., Bouwstra, J. A., Gooris, G. S., & Lee, G. (1993) *J. Controlled Release 23*, 27−36.
Schurer, N. Y., & Elias, P. M. (1991) *The Biochemistry and Function of Stratum Corneum Lipids* (Elias, P. M., Ed.) pp 27−56, Academic Press, New York.
Singer, S. J., & Nicolson, G. L. (1972) *Science 175*, 720−731.
Skarjune, R., & Oldfield, E. (1979) *Biochim. Biophys. Acta 556*, 208−218.
Squier, C. A., Wertz, P. W., & Cox, P. (1991) *Arch. Oral Biol. 36*, 647−653.
Swanbeck, G. S. (1959) *Acta Derm.-Venerol. 39 (Suppl. 43)*, 5−37.
Swartzendruber, D. C. (1992) *Semin. Dermatol. 11*, 157−161.
Thewalt, J. L., Kitson, N., Araujo, C., MacKay, A., & Bloom, M. (1992) *Biochem. Biophys. Res. Commun. 188*, 1247−1252.
Wertz, P. W., & Downing, D. T. (1989) in *Transdermal Drug Delivery* (Hadgraft, J., & Guy, R. H., Eds.) pp 1−17, Marcel Dekker, New York and Basel.
Wertz, P. W., & Downing, D. T. (1991) in *Physiology, Biochemistry and Molecular Biology in the Skin* (Goldsmith, L. A., Ed.) 2nd ed., pp 205−236, Oxford University Press, Oxford.
White, S. H., Mirejovsky, D., & King, G. I. (1988) *Biochemistry 27*, 3725−3732.
Wilkes, G. L., Nguyen, A.-L., & Wildhauer, R. (1973) *Biochim. Biophys. Acta 304*, 267−275.

BI9628127